Research Article

Received: 2 March 2015 Revised: 18 May 2015 Accepted article published: 14 July 2015 Published online in Wiley Online Library: 22 July 2015

(wileyonlinelibrary.com) DOI 10.1002/jctb.4761

ANFIS modeling for bacteria detection based on GNR biosensor

Elnaz Akbari,[a] Zolkafle Buntat,[a*] Elmira Shahraki,[b] Alireza Zeinalinezhad[c] and Mehrbakhsh Nilashi[d]

Abstract

BACKGROUND: Graphene is an allotrope of carbon with two-dimensional (2D) monolayer honeycombs. A larger detection area and higher sensitivity can be provided by a graphene based nanosenor because of its two-dimensional structure. In addition, owing to its special characteristics including electrical, optical and physical properties, graphene is a known more suitable candidate than other materials for use in sensor applications.

RESULT: In this research, a set of novel models employing field effect transistor (FET) structures using graphene has been proposed and the current–voltage (I-V) characteristics of graphene have been employed to model the sensing mechanism. An adaptive neuro fuzzy inference system (ANFIS) algorithm has been used to provide another model for the current–voltage (I-V) characteristic.

CONCLUSION: It has been observed that the graphene device experiences a large increase in conductance when exposed to *Escherichia coli* bacteria at 0–10^4 cfu mL^{-1} concentrations. Accordingly, the proposed model exhibits satisfactory agreement with the experimental data and this biosensor can detect *E. coli* bacteria providing high levels of sensitivity.

Keywords: graphene nanoribbon (GNR); *E. coli* bacteria; biosensor; field effect transistor; ANFIS; I-V characteristics

INTRODUCTION

The discovery of *Escherichia coli* bacteria in human colon goes back to 1885 and is associated with German bacteriologist Theodor Escherich. He found correlations between particular strains of the bacteria and diarrhoea and gastroenteritis in infants which was a significant finding in the public health area; hence the change of the name of the bacteria from *Bacterium Coli* to *Escherichia Coli* in his honor.[1,2] It must be noted that most *E. coli* bacteria do not cause any illness in humans, and some act to the benefit of the human body. However, several *E. coli* bacteria cause infections that are not gastrointestinal disorders, but rather those of the urinary tract.[3,4]

In *E. coli* sensing several biosensor structures have been used, such as optical biosensors, photodiode based sensing,[5] integrated waveguide biosensors[6] electro-chemical sensing techniques[7–10] or carbon nanotube biosensors based on a FET structure with very high limits of sensing.[11–14] Nonetheless, most of these experiments need the use of labels for detection; hence, a simpler method is required. Many of these biosensor fabrications are unmanageable or the limit of sensing is remarkably lower than preferred. Properties and definition of nanomaterials utilized as part of nanobiotechnology for *E. coli* sensing is recorded in Table 1.

Here, we describe a graphene based nanoelectronic sensor giving extremely sensitive bacteria (*E. coli*) detection (10 cfu mL^{-1}). In contrast to the mentioned approaches, which are time-consuming and tedious, the graphene based nano-electronic sensor offers sensitive and rapid measurement. The novelty of the approach is that, for the first time, the effect of *E. coli* detection on graphene electrical properties has been studied and formulated. Furthermore, typically, two distinct states, namely equilibrium (statistical) and non-equilibrium conditions are considered in most studies. In this research, both states have been applied in the mathematical formulation of sensor models.

Carbon-based materials have been explored extensively to accommodate advancing technology.[15–17] The discovery of a single atomic sheet of graphite layer or graphene by Andre Geim in 2004 has attracted much interest by communities of researchers and by technology due to its superb electronic properties.[18–21,20,22–25] Graphene has a very high charge carrier mobility which can exceed 200 000 $cm^2 V^{-1} s^{-1}$ at room temperature. According to experimental transport measurement results, due to the extraordinary feature of high electron mobility, graphene can serve as an extremely attractive material for use in nano-electronic devices, particularly in sensor applications.[26–29]

* Correspondence to: Zolkafle Buntat, Institute of High Voltage & High Current, Faculty of Electrical Engineering, Universiti Teknologi Malaysia, Johor Bahru, 81310 Malaysia. E-mail: zolkafle@fke.utm.my

a Institute of High Voltage & High Current, Faculty of Electrical Engineering, Universiti Teknologi Malaysia, Johor Bahru, 81310 Malaysia

b Department of Communications Engineering, University of Sistan and Baluchestan, Zahedan, Iran

c Chemistry Department, Anar Branch, Islamic Azad University, Anar, Iran

d Faculty of Computing, Universiti Teknologi Malaysia, 81310 Skudai, Johor, Malaysia

Table 1. Description and properties of nanomaterials used in nanobiotechnology for *E. coli* detection

Material	Recognition element	Signal transduction method	Pathogen	Detection range	Ref.
Quantum dots	Antibody	Fluorescence	*E. coli* O157:H7	106 cells/mL (PBS)	(52)
	Antibody	Fluorescence	*E. coli*	10^4cfu/mL	
Carbon nanotubes	Aptamer	Fluorescence	*E. coli*	10^3cfu/mL	(14)
SWNT					(53)
MWNT					(54)
					(55)
Magnetic nanoparticle	CP1	Magnetic	*E. coli* O157:H7	10^4cfu/mL (PBS-T)	(56)
					(57)
					(58)
Magnetic bead/quantum dot	Antibody	Fluorescence	*E. coli* 0157:H7	10^3cfu/mL (brain)	(59)
RuBpy doped silica	Antibody	Fluorescence	*E. coli* O157:H7	1 cell mL^{-1} (PBS)	(60)

Graphene nanoribbons (GNRs) are narrow graphene strips produced by standard lithographic techniques.

Herein, we introduce an FET biosensor modified by graphene which shows enhanced performance for measuring bacterium. Prototype FET structures have indicated excellent performance for transistors, interconnects, electromechanical switches, infrared emitters and biosensors.[30,31] As can be seen in Fig. 1, it looks similar to the electrolyte-gated field-effect transistor and a graphene channel connects the source and drain electrodes.[32,33] When *E. coli* bacteria come into contact with the surface or edge of graphene, the amount of carrier concentration changes due to the variability of the drain source current which is a measurable parameter. According to the relation between conductivity and charge carrier density or carrier mobility, the adsorbed molecules change the conductivity of the graphene.[34−37]

In addition to the analytical model, an adaptive neuro fuzzy inference system (ANFIS) algorithm has been developed.

EXPERIMENTAL

A chemical vapor deposition (CVD) method using ethanol was used to grow graphene film on copper foil. It was coated with a thin layer of poly-methyl methacrylate (PMMA) dissolved in chlorobenzene. Then by using a chemical etching method the graphene/PMMA was released from the copper foil. The drain and source (two electrodes) were prepared and connected to the graphene using silver. Lastly, for electrode insulation silicon rubber was used.[4]

Escherichia coli (K12 ER2925) was bought from New England Biolab and cultured in LB (Luria Bertani) medium at 37 °C. Culturing and colony counting methods were used for *E. coli* production at 10^7 cfu mL^{-1} density. It was prepared for experimental work by diluting it in PBS solution (PH 7.2). The harvested *E. coli* was stored at −80 °C. A semiconductor device analyzer was used for electrical measurement (Agilent, B1500A) and all measurements were done under ambient conditions. The gate voltage was applied via an Ag/AgCl electrode immersed in PBS solution on top of the graphene and the graphene device was biased at 100 mV.[4]

PROPOSED MODEL

An *E. coli* in contact with a film of antibody functionalized graphene is illustrated in Fig. 1. In this configuration, to check the system response and to find the kinetics of bacteria binding, the sensor was kept in chambers with 10^4 cfu mL^{-1} of *E. coli*.[4,38] As higher numbers of *E. coli* are caught by the graphene film antibodies, the conductance of the channel increases. Operating the graphene FET in the p-type region with zero gate voltage confirms that the graphene conductance increases as a result of higher levels of hole density caused by the high negativity of the walls of the bacteria.

It has been proved by experimental methods that the conductance of graphene is a function of carrier density and mobility. In other words, changes in electron density and/or charge carriers by adsorption of *E. coli* molecules or ions in graphene change the conductance:[39]

We begin the modelling by carrier concentration given as:[40,41]

$$n = \int D(E) f(E) d(E) \tag{1}$$

where $f(E)$ is Fermi Dirac distribution and $D(E)$ the density of state (DOS) and can be written as:[40]

$$D(E) = \frac{1}{3\pi t a_{c-c}} \frac{E}{\sqrt{E^2 - \left(\frac{E_g}{2}\right)^2}} \tag{2}$$

in which $a_{C-C} = 1.42$ Årepresents carbon−carbon (C−C) bond length, and $t = 2.7$ (eV) is the nearest neighbour C−C tight binding overlap energy. E_g is the band gap energy which can be written for monolayer graphene as:[42,43]

$$E_g = 2\pi\sqrt{3}\left(\frac{p}{N+1} - \frac{2}{3}\right) \tag{3}$$

in which p signifies an integer number, and the Fermi Dirac distribution $f(E)$ is defined as:[44]

$$f(E) = \frac{1}{\exp\left(\frac{E-E_F}{k_B T}\right) + 1} \tag{4}$$

where E_F is Fermi energy, K_B is Boltzmann's constant, T is temperature and E is energy. Then the *E. coli* concentration is written as:

$$n = \int \frac{1}{3\pi t a_{c-c}} \frac{E}{\sqrt{E^2 - \left(\frac{E_g}{2}\right)^2}} \cdot \frac{1}{\exp\left(\frac{E-E_F}{k_B T}\right) + 1} .d(E) \tag{5}$$

The quantum capacitance is shown as:[45]

$$C_q = \frac{\delta Q}{\delta V} \tag{6}$$

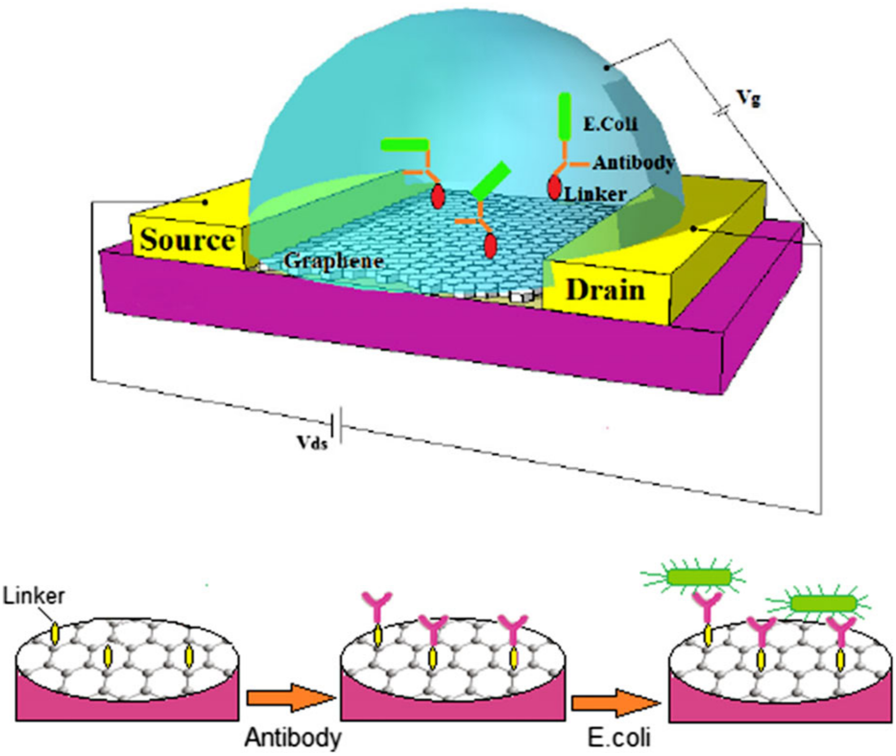

Figure 1. Graphene-FET for detection of *E. coli*.

in which Q is the charge measured in coulombs and $\delta Q = e.\delta n_{Total}$, e is electron charge, $n_{Total} = n + n'$, where n is inherent carrier concentration and n' is the amount of carrier concentration when bacteria is injected.

$\partial V = \frac{\partial E}{e}$ is the voltage applied to the device and C_q is given as:[46]

$$C_q = \frac{e\partial n_{Total}}{\frac{\partial E}{e}} \tag{7}$$

which becomes by a simple mathematical rearrangement:

$$C_q = e^2 \frac{\partial n_{Total}}{\partial E} \tag{8}$$

Using the definition of n_{Total}, the following equation can be written for quantum capacitance:

$$C_q = e^2 \frac{\partial n}{\partial E} + e^2 \frac{\partial n'}{\partial E} \tag{9}$$

The performance of a biosensor based on graphene nanostructure is demonstrated by its conductance characteristic. As V_g results in altering the conductance of the channel, one of the parameters that has strong influence on biosensor conductance is *E. coli* concentration, so we can write:

$$n' = \psi F_{EC} \tag{10}$$

where (F_{EC}) is the carrier concentration of *E. coli* and the control parameter is indicated by (ψ). As a result, the quantum capacitance can be written as:

$$C_q = e^2.\frac{1}{3\pi t a_{c-c}} \frac{E}{\sqrt{E^2 - \left(\frac{E_g}{2}\right)^2}}.\frac{1}{\exp\left(\frac{E-E_F}{k_B T}\right) + 1} + e^2 \frac{\partial F_{EC}}{\partial t}\frac{\partial t}{\partial E} \tag{11}$$

The GFET conductance can be written as follows:

$$G = \left(e^2.\frac{1}{3\pi t a_{c-c}} \frac{E}{\sqrt{E^2 - \left(\frac{E_g}{2}\right)^2}}.\frac{1}{\exp\left(\frac{E-E_F}{k_B T}\right) + 1} + e^2 \psi \frac{\partial F_{EC}}{\partial t}\frac{\partial t}{\partial E} \right) .V_{ds}.\mu_e \tag{12}$$

Based on the analytical model, ψ is introduced as the *E. coli* controlled parameter and shows the rate of change in conductivity depends on *E. coli* concentration that is given by:

$$\psi = \mathrm{aLn}\ \left(F_{EC}\right)\ + \mathrm{b} \tag{13}$$

where the constant parameters have been calculated as a = 57550 and b = 18848.

ANFIS MODEL

Fuzzy logic (FL) and fuzzy inference systems (FIS), first proposed by Zadeh (1965), provide a solution for making decisions based on vague, ambiguous, imprecise or missing data. FL represents models or knowledge using IF–THEN rules. A neuro-fuzzy system is functionally equivalent to a FIS. A FIS mimics a human reasoning process by implementing fuzzy sets and approximate reasoning mechanism which use numerical values instead of logical values. A FIS requires a domain expert to define the MFs and to determine the associated parameters both in the MFs, and the reasoning section. However, there is no standard for the knowledge acquisition process and thus the results may be different if a different knowledge engineer is at work in acquiring the knowledge from experts. A Neuro-Fuzzy system can replace

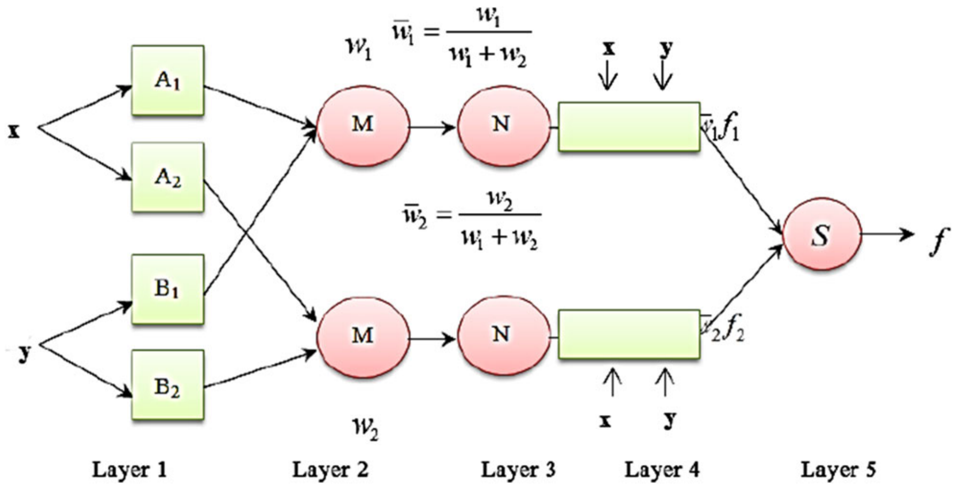

Figure 2. ANFIS architecture.

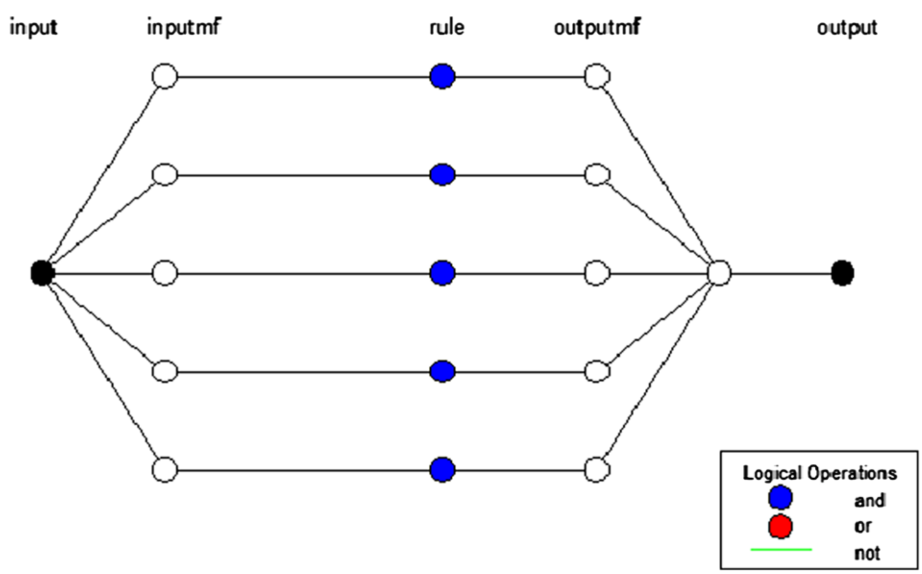

Figure 3. Schematic of implemented ANFIS.

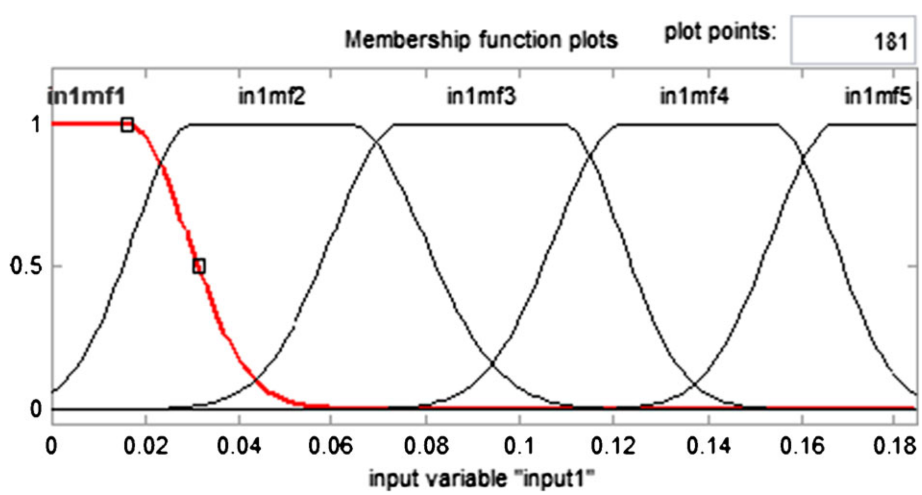

Figure 4. Membership functions.

Table 2. MFs ranges

Cfu mL^{-1}	In1mf1	In1mf2	In1mf3	In1mf4	In1mf5
0	0.008462–0.01495 0.01486–0.01832	.01433–0.03209 0.01469–0.06739	0.01538–0.08101 0.01498–0.1177	0.01481–0.1316 0.01307–0.1659	0.01438–0.1809 0.008462–0.2142
10	0.008462–0.01495 0.01499–0.01845	0.01336–0.03282 0.01496–0.06784	0.01575–0.08103 0.01489–0.1176	0.01477–0.1314 0.01276–0.166	0.01471–0.1808 0.008462–0.2142
100	0.008493–0.015 0.01475–0.0182	0.01364–0.03241 0.0162–0.06944	0.01456–0.0827 0.01575–0.1189	0.01334–0.1333 0.0126–0.1674	0.01522–0.1821 0.008493–0.215
1000	0.0084–0.0141 0.01504–0.01902	0.0.01327–0.03302 0.0144–0.06752	0.01431–0.08198 0.01447–0.1173	0.01629–0.1303 0.01384–0.1664	0.01354–0.1811 0.0084–0.2134
10000	0.007842–0.01385 0.0127–0.0163	0.01259–0.0301 0.01579–0.06372	0.0147–0.07481 0.01273–0.1089	0.01441–0.1219 0.01257–0.1539	0.01365–0.1673 0.007842–0.1985

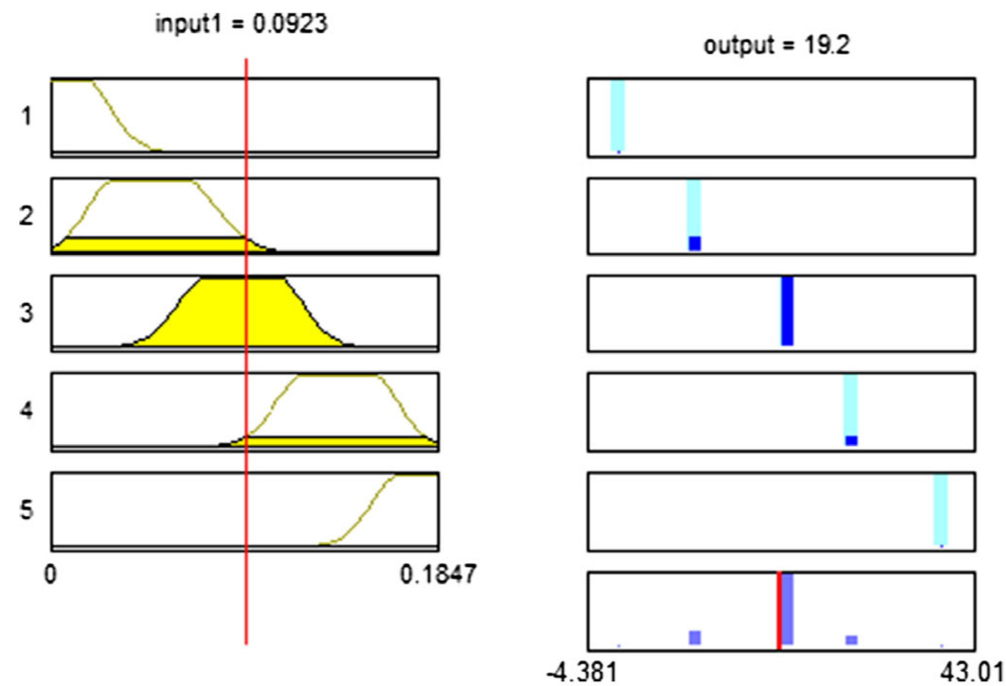

Figure 5. Fuzzy rule viewer for input and output variables of ANFIS model.

the knowledge acquisition process by humans using a training process with an input–output training dataset. Thus instead of being dependent on human experts the Neuro-Fuzzy system will determine the associated parameters through a training process, by minimizing an error criterion. A popular Neuro-Fuzzy system is an ANFIS, a fuzzy system that uses an artificial neural network theory to determine its properties (fuzzy sets and fuzzy rules).[47,48]

The main objective of ANFIS modeling is to map the inputs to outputs to find a function $\hat{f}$ for a given input vector $X = (x_1, x_2, x_3, \ldots, x_n)$ in order to predict output $\hat{y}$ as close as possible to its actual output$y$. Assume m observations of multi-input–single-output data pairs is available such as $X = (x_{i1}, x_{i2}, x_{i3}, \ldots, x_{in})$, and

$$y_i = f\left(x_{i1}, x_{i2}, x_{i3}, \ldots, x_{in}\right) \; i = 1, 2, \ldots, m \tag{14}$$

It is now possible to build a model using ANFIS in a prediction task for any given new input vector$X = (x_{i1}, x_{i2}, x_{i3}, \ldots, x_{in})$. This prediction,$\hat{y}_i$ is an approximation of $y$that can be presented as

$$\hat{y}_i = \hat{f}\left(x_{i1}, x_{i2}, x_{i3}, \ldots, x_{in}\right) \; i = 1, 2, \ldots, m \tag{15}$$

The goal is to minimize the difference between the actual output and the predicted one by determining an ANFIS model.

$$\sum_{i=1}^{m} \left[\hat{f}\left(x_{i1}, x_{i2}, x_{i3}, \ldots, x_{in}\right) - y_i\right]^2 \rightarrow \min . \tag{16}$$

Indeed, in ANFIS the linguistic Takagi and Sugeno (TSK) type fuzzy IF-THEN rules are used for prediction task. These rules are generated by training the model to approximate f by $\hat{f}$ using m observations of n-input–single-output data pairs (x_i, y_i). ANFIS is a structure that consists of nodes and directional links through which the nodes are connected. A back-propagation strategy is used to train the MFs, while the least mean squares algorithm determines the coefficients of the linear combinations in the consequent part of the model. TSK type fuzzy IF-THEN rules are used in the ANFIS model, for example:

$$if\ \left(x\ is\ A_1\right)\ and\ \left(y\ is\ B_1\right),\ then\ f_1 = p_1 x + q_1 y + r_1,$$

$$if\ \left(x\ is\ A_2\right)\ and\ \left(y\ is\ B_2\right),\ then\ f_2 = p_2 x + q_2 y + r_2,$$

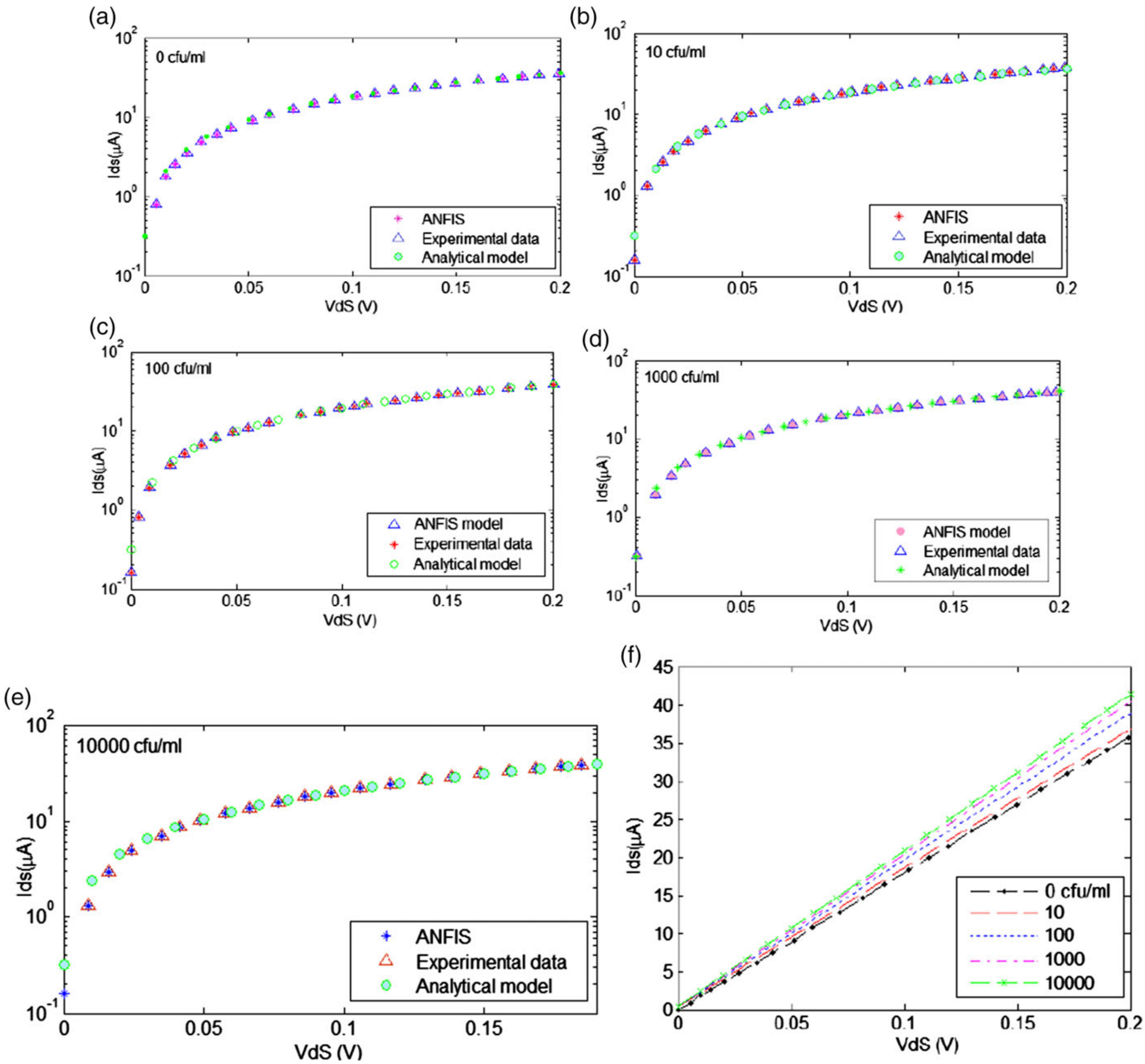

Figure 6. Current–voltage characteristics for different *E. coli* concentrations.

where x and y are the inputs, f_i is the output, p_i , q_i and r_i are the design parameters that are determined by the users during the training process. A_i and B_i are the fuzzy sets according to predefined MF. An ANFIS model with two inputs and two fuzzy rules is implemented in Fig. 2.

Bacteria biosensor prediction using the ANFIS model

Fuzzy logic (FL) and fuzzy inference systems (FIS), first proposed by Zadeh in 1965, provide a solution for making decisions based on vague, ambiguous, imprecise or missing data. FL represents models or knowledge using IF–THEN rules.

Neural networks learn system behavior by using system input–output data. Neural networks have good generalization capabilities. The learning and generalization capabilities of neural networks enable it to more effectively address real-world problems. Thus, neural networks can solve many problems that are either unresolved or inefficiently solved by existing techniques, including fuzzy logic.[27]

Both fuzzy logic and neural networks have been very successful in solving many real-world problems. However, both technologies have some limitations. In fuzzy logic, it is usually difficult to determine the correct set of rules and membership functions. Moreover, fine-tuning a fuzzy solution is even more difficult and takes longer. In neural networks, it is difficult to understand the 'Black Box,' i.e. it is incomplete compared with a fuzzy rule based system description.

An appropriate combination of these two technologies (Neuro-Fuzzy) can effectively solve the problems of fuzzy logic and neural networks. A Neuro-Fuzzy approach was used to take advantage of the neural network's ability to learn, and the membership degrees and functions of fuzzy logic. The weights of the neural networks are mapped to fuzzy logic rules and member

Table 3. ψ parameter corresponding to *E. coli* concentration values

F(cfu mol^{-1})	Ψ(Constant)
0	0.7
10	0.72
100	0.75
1000	0.78
10000	0.8

functions. Expressing the weights of the neural network by fuzzy rules also provides a better understanding of the 'Black Box' and thus helps to better design the neural network itself. Thus, while the learning of neural network is parameterized by the variation in input data, the learning of ANFIS is fixed by the rules and membership function values that we define.

In this paper, we develop a Neuro-Fuzzy system for pre cutting the biosensor conductance variation. Generating the proper MFs and extracting the fuzzy rules for the prediction of overall ratings are the main advantages of this method for the defined problem.

Hence, in this study, discovering the knowledge (fuzzy rules) from experimental data and generalizing the relationship $Y = f(X_1)$ are the main goals of applying ANFIS for accurate prediction of conductance. In this relationship, X_1 stands for input variable and Y stands for output variable. In the current study, conductance can be determined as a function of voltage. Predicting the relationship between inputs and output is one of the important tasks that ANFIS does. Figure 3 shows the architecture of the implemented ANFIS that consists of 1 input, 5 rules, and 5 MFs for inputs and output.

After implementing the ANFIS model using the fuzzy logic toolbox in Matlab software, the training was tested for error estimation. Data from one input was given to a trained model of ANFIS along with actual output. From the input values, suitable MFs (Fig. 4) were selected to predict the output using the extracted rules.

In Table 2, the range of MFs for all prediction models developed by ANFIS are presented. As can be seen from this table, Gaussian MFs were selected for the models. These ranges and MF types were selected as they minimize the errors of prediction.

From the fuzzy rule viewer of the ANFIS model established shown in Fig. 5, the process of biosensor prediction by selecting the MFs can be better visualized. From the fuzzy rule viewer above, when the input parameter is at 0.0923, an output of voltage at 19.2 is obtained.

RESULTS

To check their functionality, the graphene devices were kept in closed chambers with various *E. coli* concentrations to allow the bacteria to grow and multiply. The graphene devices were then washed with a PBS solution of pH 7.2 (to allow for the production of the intended final *E. coli* concentration)[4] and were electrically tested through measuring the I–V characteristics with zero voltage between the solution and the gate. The current–voltage characteristics of the proposed model for a biosensor based on graphene in comparison with results from experimental data and the ANFIS model are illustrated in Fig. 6(a) to 6(f). It can be observed that the charge transfer between *E. coli* (0 to 10 000 cfu mol^{-1}) and graphene causes the current to increase. An acceptable agreement between extracted data and the suggested model is clearly illustrated in the figures. In the proposed model, different amounts of *E. coli* concentration are shown in term of control parameter (ψ) as presented in Table 3.

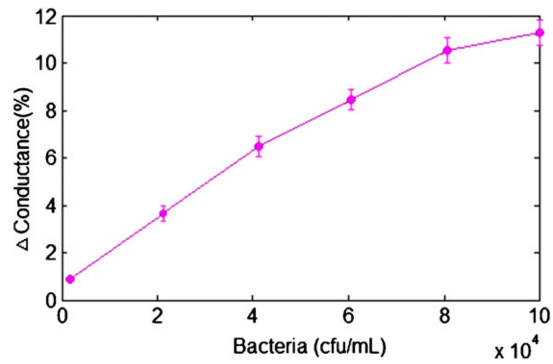

Figure 7. Plot of device conductance versus *E. coli* concentration. Averages of the values from six devices are taken for each data point and the corresponding standard errors are represented by error bars.

Figure 7 shows the conductance of graphene at several different bacteria concentrations.

As can be seen, a concentration of *E. coli* as low as 10 cfu mL^{-1} was detected by the graphene based sensor. This is several orders better than the sensitivity of formerly stated approaches such as SWCNT-network FETs,[49] polymerase series response,[50] and external plasmon intensification.[51] 10 cfu mL^{-1} of *E. coli* created a 3.25 ± 0.43% increase in the conductance of the graphene based sensor (n =6 devices) which relates to an increase of ∼1.17 μA at Vds = 0.2 V (notably greater than the existing noise of 0.02 μA).

CONCLUSION

The graphene component shows measureable changes in conductance when in contact with *E. Coli*, and this behavior is proposed to be used for the detection of this type of bacteria. A bacteria concentration control parameter (ψ) is introduced in the derivation of the analytical model and is calculated iteratively. The sensor created is label-free, rapid, extremely sensitive and selective for the detection of bacteria *E. Coli*, with a very low sensing limit of 10 cfu mL^{-1}. Comparison between the results obtained from the analytical and ANFIS models enables more accurate estimations. With the aid of the proposed models, a realistic understanding of the biosensor performance under exposure to *E. coli* can be gained minimizing the need for empirical experiments.

ACKNOWLEDGEMENT

The authors would like to thank Ministry of Higher Education (MOHE), Malaysia (grant Vot. No. 4F382) and the Universiti Teknologi Malaysia (grants Vot. No. 03H86 and Vot. No. 04H40) for the financial support received during the investigation.

REFERENCES

1 Anthony M, *Computational Learning Theory*. Cambridge University Press (1997).
2 Wittstock A, Biener J and Erlebacher J Eds, Nanoporous gold: from an ancient technology to a high-tech material. *Royal Soc Chem* DOI: 10.1039/9781849735285 (2012).
3 Stahlbock R and Lessmann S, *Potential von Support Vektor Maschinen im analytischen Customer Relationship Management*. Universität Hamburg, Hamburg, Arbeitspapier. 2004.

4 Huang Y, Dong X, Liu Y, Li L-J and Chen P, Graphene-based biosensors for detection of bacteria and their metabolic activities. *J Mater Chem* **21**:12358–12362 (2011).
5 Song JM and Kwon HT, Photodiode array on-chip biosensor for the detection of *E. coli* O157: H7 pathogenic bacteria. In *Biosensors and Biodetection*. Springer, 325–335 (2009).
6 Zhu P, Shelton DR, Karns JS, Sundaram A, Li S, Amstutz P, *et al.*, Detection of water-borne *E. coli* O157 using the integrating waveguide biosensor. *Biosens Bioelectron* **21**:678–683 (2005).
7 Zhang X, Geng P, Liu H, Teng Y, Liu Y, Wang Q, *et al.*, Development of an electrochemical immunoassay for rapid detection of *E. coli* using anodic stripping voltammetry based on Cu@ Au nanoparticles as antibody labels. *Biosens Bioelectron* **24**:2155–2159 (2009).
8 Liao JC, Mastali M, Li Y, Gau V, Suchard MA, Babbitt J, *et al.*, Development of an advanced electrochemical DNA biosensor for bacterial pathogen detection. *J Mol Diagnost* **9**:158–168 (2007).
9 Yang L and Bashir R, Electrical/electrochemical impedance for rapid detection of foodborne pathogenic bacteria. *Biotechnol Adv* **26**:135–150 (2008).
10 Chang L, Liu C, He Y, Xiao H and Cai X, Small-volume solution current-time behavior study for application in reverse iontophoresis-based non-invasive blood glucose monitoring. *Sci China Chem* **54**:223–230 (2011).
11 Vashist SK, Zheng D, Al-Rubeaan K, Luong JH and Sheu F-S, Advances in carbon nanotube based electrochemical sensors for bioanalytical applications. *Biotechnol Adv* **29**:169–188 (2011).
12 García-Aljaro C, Cella LN, Shirale DJ, Park M, Muñoz FJ, Yates MV, *et al.*, Carbon nanotubes-based chemiresistive biosensors for detection of microorganisms. *Biosens Bioelectron* **26**:1437–1441 (2010).
13 Zhang X, Wang D, Yang D, Li S and Shen Z, Electronic detection of escherichia coli O157: H7 using single-walled carbon nanotubes field-effect transistor. *Biosensor Eng* **4**:94 (2013).
14 Villamizar RA, Maroto A, Rius FX, Inza I and Figueras MJ, Fast detection of *Salmonella Infantis* with carbon nanotube field effect transistors. *Biosens Bioelectron* **24**:279–283 (2008).
15 Balabin RM and Lomakina EI, Support vector machine regression (SVR/LS-SVM) – an alternative to neural networks (ANN) for analytical chemistry? Comparison of nonlinear methods on near infrared (NIR) spectroscopy data. *Analyst* **136**:1703–1712 (2011).
16 Goh M and Pumera M, Graphene-based electrochemical sensor for detection of 2,4,6-trinitrotoluene (TNT) in seawater: the comparison of single-, few-, and multilayer graphene nanoribbons and graphite microparticles. *Analyti Bioanalyt Chem* **399**:127–131 (2011).
17 Akbari E, Arora VK, Enzevaee A, Ahmadi MT, Khaledian M and Yusof R, Gas concentration effects on the sensing properties of bilayer graphene. *Plasmonics* **9**(4):987–992 (2014).
18 Yuan W and Shi G, Graphene-based gas sensors. *J Mater Chem A* **1**(35):10078–10091 (2013).
19 Wang Q and Arash B, A review on applications of carbon nanotubes and graphenes as nano-resonator sensors. *Comput Mater Sci* **82**:350–360 (2014).
20 Gunn SR, Support vector machines for classification and regression. ISIS Technical Report. 14 (1998).
21 Nguyen HB, Nguyen VC, Nguyen VT, Le HD, Nguyen VQ, Ngo TTT, *et al.*, Development of the layer-by-layer biosensor using graphene films: application for cholesterol determination. *Adv Natural Sci: Nanosci Nanotechnol* **4**:015013 (2013).
22 Smola AJ and Schölkopf B, A tutorial on support vector regression. *Statist Comput* **14**:199–222 (2004).
23 Novoselov KS, Fal V, Colombo L, Gellert P, Schwab M and Kim K, A roadmap for graphene. *Nature* **490**:192–200 (2012).
24 Pumera M, Polsky R and Banks C, Graphene in analytical science. *Analyt Bioanalyt Chem* **406**:6883–6884 (2014).
25 Nguyen HB, Nguyen VC, Nguyen VT, Ngo TTT, Nguyen NT, Dang TTH, *et al.*, Graphene patterned polyaniline-based biosensor for glucose detection. *Adv Natural Sci: Nanosci Nanotechnol* **3**:025011 (2012).
26 Specht DF, A general regression neural network. *Neural Networks, IEEE Trans* **2**:568–576 (1991).
27 Falkovsky L, Physical properties of graphene. *Uspekhi Fizicheskikh Nauk* **182**:1223–1234 (2012).
28 Schölkopf B, Burges CJ and Smola AJ, *Advances in Kernel Methods: Support Vector Learning*. MIT Press (1999).
29 Liu Z, Liu B, Ding J and Liu J, Fluorescent sensors using DNA-functionalized graphene oxide. *Analyt Bioanalyt Chem* **406**:6885–6902 (2014).
30 Foxe M, Lopez G, Childres I, Jalilian R, Roecker C, Boguski J, *et al.*, Detection of ionizing radiation using graphene field effect transistors. In *IEEE Nuclear Science Symposium Conference Record*, Vols **1-5**, ed by Yu B, 2009.
31 Ohno Y, Maehashi K and Matsumoto K, Graphene field-effect transistors for label-free biological sensors. In *IEEE Sensors*, 2010, 903–906.
32 Hasegawa M, Hirayama Y, Ohno Y, Maehashi K and Matsumoto K, Characterization of reduced graphene oxide field-effect transistor and its application to biosensor. *Japanese J Appl Phys* **53**(5S1):05FD (2014).
33 Schwierz F, Graphene transistors. *Nat Nano* **5**:487–496 (2010).
34 Neto AC, Guinea F, Peres N, Novoselov KS and Geim AK, The electronic properties of graphene. *Rev Modern Phys* **81**:109 (2009).
35 Fang M, Wang K, Lu H, Yang Y and Nutt S, Covalent polymer functionalization of graphene nanosheets and mechanical properties of composites. *J Mater Chem* **19**:7098–8105 (2009).
36 North S, Lock E, Taitt C and Walton S, Critical aspects of biointerface design and their impact on biosensor development. *Analyt Bioanalyt Chem* **397**:925–933 (2010).
37 Caucheteur C, Guo T and Albert J, Review of plasmonic fiber optic biochemical sensors: improving the limit of detection. *Analyt Bioanalyt Chem* **2015**:1–15 (2015).
38 Welling M, *Support vector regression*. Department of Computer Science, University of Toronto, Toronto (Canada). 2004.
39 Ahmadi MT, Johari Z, Amin NA, Fallahpour AH and Ismail R, Graphene nanoribbon conductance model in parabolic band structure. *J Nanomater* **2010**:12 (2010).
40 Lundstrom M and Guo J, *Nanoscale Transistors: Device Physics, Modeling and Simulation*. Springer Science and Business Media (2006).
41 Marulanda JM and Srivastava A, Carrier density and effective mass calculations in carbon nanotubes. *Physica Status Solidi (b)* **245**:2558–2562 (2008).
42 Wong H-SP and Akinwande D, *Carbon Nanotube and Graphene Device Physics*. Cambridge University Press (2010).
43 Ismail R, Ahmadi MT and Anwar S, *Advanced Nanoelectronics*. CRC Press (2012).
44 Datta S, *Quantum Transport: Atom to Transistor*. Cambridge University Press (2005).
45 Xia J, Chen F, Li J and Tao N, Measurement of the quantum capacitance of graphene. *Nature Nanotechnol* **4**:505–509 (2009).
46 Shylau A, Kłos J and Zozoulenko I, Capacitance of graphene nanoribbons. *Phys Rev B* **80**:205402 (2009).
47 Nilashi M, bin Ibrahim O and Ithnin N, Multi-criteria collaborative filtering with high accuracy using higher order singular value decomposition and Neuro-Fuzzy system. *Knowledge-Based Syst* **60**:82–101 (2014).
48 Nilashi M, bin Ibrahim O and Ithnin N, Hybrid recommendation approaches for multi-criteria collaborative filtering. *Expert Syst Applications* **41**:3879–3900 (2014).
49 Dong X, Long Q, Wang J, Chan-Park MB, Huang Y, Huang W, *et al.*, A graphene nanoribbon network and its biosensing application. *Nanoscale* **3**:5156–5160 (2011).
50 Taylor AD, Ladd J, Yu Q, Chen S, Homola J and Jiang S, Quantitative and simultaneous detection of four foodborne bacterial pathogens with a multi-channel SPR sensor. *Biosens Bioelectron* **22**:752–758 (2006).
51 Wang Y, Ye Z and Ying Y, New trends in impedimetric biosensors for the detection of foodborne pathogenic bacteria. *Sensors* **12**:3449–3471 (2012).
52 Tully E, Hearty S, Leonard P and O'Kennedy R, The development of rapid fluorescence-based immunoassays, using quantum dot-labelled antibodies for the detection of *Listeria monocytogenes* cell surface proteins. *Int J Biologic Macromol* **39**:127–134 (2006).
53 Cella LN, Chen W, Myung NV and Mulchandani A, Single-walled carbon nanotube-based chemiresistive affinity biosensors for small molecules: ultrasensitive glucose detection. *J Am Chem Soc* **132**:5024–5026 (2010).
54 Lei J and Ju H, Nanotubes in biosensing. *Wiley Interdisciplinary Rev: Nanomed Nanobiotechnoly* **2**:496–509 (2010).
55 Cheng Y, Liu Y, Huang J, Li K, Xian Y, Zhang W, *et al.*, Amperometric tyrosinase biosensor based on Fe 3 O 4 nanoparticles-coated carbon nanotubes nanocomposite for rapid detection of coliforms. *Electrochimica Acta* **54**:2588–2594 (2009).
56 So HM, Park DW, Jeon EK, Kim YH, Kim BS, Lee CK, *et al.*, Detection and titer estimation of *Escherichia coli* using aptamer-functionalized

single-walled carbon-nanotube field-effect transistors. *Small* **4**:197–201 (2008).
57 Liébana S, Lermo A, Campoy S, Barbé J, Alegret S and Pividori MI, Magneto immunoseparation of pathogenic bacteria and electrochemical magneto genosensing of the double-tagged amplicon. *Analyt Chem* **81**:5812–5820 (2009).
58 Mujika M, Arana S, Castano E, Tijero M, Vilares R, Ruano-Lopez J, *et al.*, Magnetoresistive immunosensor for the detection of *Escherichia coli* O157: H7 including a microfluidic network. *Biosens Bioelectron* **24**:1253–1258 (2009).
59 Yang L and Li Y, Simultaneous detection of *Escherichia coli* O157: H7 and *Salmonella Typhimurium* using quantum dots as fluorescence labels. *Analyst* **131**:394–401 (2006).
60 Su X-L and Li Y, Quantum dot biolabeling coupled with immunomagnetic separation for detection of *Escherichia coli* O157: H7. *Analyt Chem* **76**:4806–4810 (2004).

